TRIDYN

1D Dynamic Computer Simulation of Ion Irradiation Processes Using the Binary Collision Approximation

User Guide

Wolfhard Möller

Institute of Ion Beam Physics and Materials Research
Helmholtz-Zentrum Dresden-Rossendorf
01314 Dresden, Germany

List of contents

1. Introduction

TRIDYN allows to simulate fast ion irradiation effects and thin-film deposition on semi-infinite bodies and free-supported thin films with flat surfaces. Collisional processes, being modelled in the binary collision approximation (BCA), include the deposition, implantation and scattering of the incoming atoms, the formation of collisional cascades and the related formation of point defect damage, ion mixing, and sputtering of atoms from the surface. In "dynamic" mode, the code models the dynamic alteration of the material under irradiation due to the deposition or implantation of incident atoms, due to atomic relocation in the bulk and due to sputter erosion at the surface. In this way, e.g., high-fluence implantation profiles, ion-assisted deposition of thin films and ion erosion can be described.

In BCA, the history of the incident ions and the development of collision cascades is modelled as a sequence of binary collisions. Compared to more elaborate simulation procedures, as, e.g., of the molecular dynamics (MD) type, BCA is restricted to particle energies well above the characteristic binding energies of a solid (several eV), but the computational speed is vastly larger. Depending on the actual problem, typical simulation times range from a few seconds to a few hours on a present-day personal computer or on a low-cost workstation.

After the first static BCA codes had been programmed for crystalline materials about 50 years ago[1], a worldwide breakthrough was achieved with the TRIM (TRansport of Ions in Matter) code for amorphous substances[2-4]. The original TRIM program was designed for the calculation of ion stopping and ranges only. A version including the treatment of secondary recoil cascades and the associated collisional sputtering (TRIM.SP) was developed later[5]. This option has also been added to the TRIM simulation section of the SRIM (Stopping and Ranges of Ions in Matter) package, which offers also quick transport theory calculations of ion stopping and ranges. SRIM is available as freeware, which is maintained up to date, and can be run under Windows with a convenient user interface (see www.srim.org). There are, however, limitations to the application of the TRIM code:

(i)   Although the collisional algorithms work in three dimensions, TRIM describes only one-dimensional target materials with a flat surface.
(ii) Any dynamic alteration of the material due to ion implantation, atomic relocation and sputtering is not taken into account.
(iii) There are well-known deficiencies in the detailed description of sputtering (as, e.g., multicomponent sputtering, angular distributions of sputtered atoms).

The present program (for earlier versions, see refs.[6, 7]) originates from the early TRIM.SP code mentioned above. It has been developed, revised and extended at Max-Planck-Institute of Plasma Physics (IPP) and the present Helmholtz-Zentrum Dresden-Rossendorf (HZDR). Follow-up versions include fully two-dimensional (IPP: "SDTrimSP-2D"[8]) and three-dimensional (HZDR: "TRI3DYN"[9]) dynamic modifications. Further, a fast static 3D versions ("TRI3DST") has recently been created at HZDR.

The present User Guide contains a short description of the program, followed by operation instructions including a detailed description of the input and output data.

2. Computational volume and body

A 3D Cartesian coordinate system (x, y, z) is employed for the slowing down of incident projectiles and the development of collision cascades where x points into the depth. The computational volume is setup within $x = 0 \dots x_{max}$ and is laterally unlimited in y and z direction. The initial computational body is defined as a multilayered structure with N_x equisized depth intervals of spacing $\Delta x_0 = x_{max}/N_x$, and may be set up either as a semi-infinite structure (see Fig. 2.1) or as a free-supported

thin film of thickness d_{thf} (see Fig. 2.2). The initial thickness of each layer within these structures is a multiple of Δx_0. During dynamic relaxation, the internal depth spacing becomes non-equidistant.
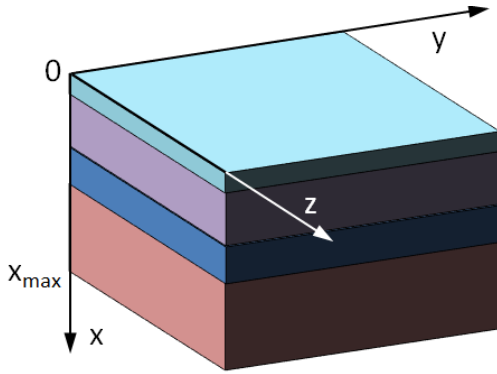
Figure 2.1: Example of a layered semi-infinite body with $0 \leq x \leq x_{max}$ and $-\infty < y, z < +\infty$. The thickness of each layer is a multiple of the initial depth spacing Δx_0. The color indicates different local compositions (here, a three-layer system on top of a substrate).

Figure 2.2: Example of a layered free-supported thin film structure with the film thickness d_{thf}, $0 \leq x \leq x_{max}$ and $-\infty < y, z < +\infty$. The empty space at the bottom assures a correct treatment of transmitted atoms. See Fig. 2.1 for further explanation.
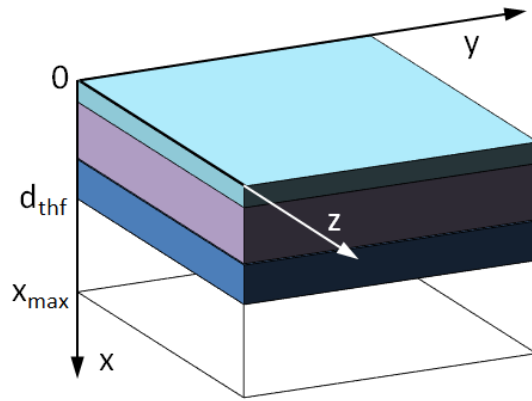
3. Areal density and local composition

With N_c different atomic species being present in the body, the local composition in each depth interval of thickness Δx can be defined by the partial atomic areal densities v_l ($l = 1 \dots N_c$) with

$$\sum_{l=1}^{N_c} v_l = \begin{cases} 0 & if\ interval\ is\ empty \\ v & else \end{cases} \tag{3.1}$$

with v denoting the total areal densities. The atomic fractions in each depth interval (which are used by the program for input and output of the compositional profiles only) are

$$q_l = \begin{cases} 0 & if\ interval\ is\ empty \\ v_l/v & else \end{cases} \tag{3.2}$$

In the relaxed state, each atom fills its predefined atomic volume according to

$$\Delta x = \sum_{l=1}^{N_c} \frac{v_l}{n_l^0} \tag{3.3}$$

where n_l^0 denote the inverse of the atomic volumes of the components l. n_l^0 can be automatically taken as the atomic densities of the pure components, or be adjusted so that

$$\frac{1}{n} = \sum_{l=1}^{N} \frac{q_l}{n_l^0}$$

(3.4)

correctly describes the total atomic density n of some compound of N elements. Optionally, n_l^0 can be defined automatically for a list of selected binary compounds which is embedded in the program. (See also Appendix A3)

4. Irradiation and Deposition

TRIDYN allows a simultaneous multispecies irradiation/deposition of/on the top surface, which is defined by up to 10 different irradiation conditions. Each condition carries the species of the projectile, its energy and the angle of irradiation. Specific parameters may be assigned to each irradiation/deposition condition.

For each condition, the directional unity vector of incidence, $\overrightarrow{d_{inc}}$, is defined by the polar angle α with respect to the x axis, as shown in Fig. 4.1. In TRIDYN, the plane of incidence is the $y - z$ plane. All projectiles start at $(x, y, z) = (0,0,0)$. Their exact launching point, however, is randomly varied along $\overrightarrow{d_{inc}}$ within the mean collisional free pathlength (see sect. 7).
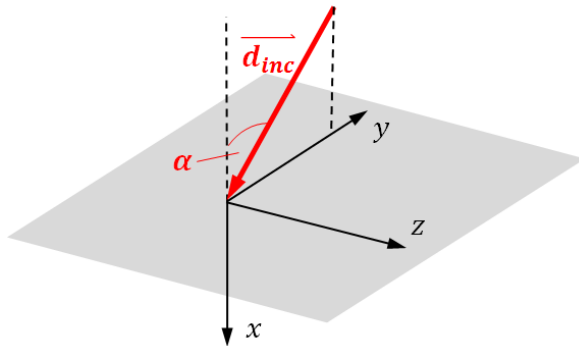
Figure 4.1: Directional vector $\overrightarrow{d_{inc}}$ and the polar angle α of irradiation in relation to the coordinate system. The plane of incidence is the $x - y$ plane. All projectiles start at $(x, y, z) = (0,0,0)$.

Optionally, the direction of incidence may be blurred around the mean direction $\overrightarrow{d_{inc}}$ by means of selected two-dimensional angular distributions, which are described in detail in Appendix B.

For each irradiation condition, a fixed energy of incidence may optionally be replaced by a random choice of the actual energy from a predefined energy distribution, or a linear ramp of the energy.

5. The pseudoatom concept; statistical quality of the simulation

The dynamic simulation of the transport of moving atoms (projectiles or generated recoil atoms) employs pseudoatoms which represent a certain areal density of real atoms which is defined by

$$\psi_0 = \frac{\phi_0}{N_p^0}$$

(5.1)

where ϕ_0 denotes the total fluence of incident projectiles for the simulation run, and N_p^0 the number of incident pseudoprojectiles. The statistical quality of the simulation improves at increasing N_p^0, i.e. at decreasing ψ_0, for a predefined total fluence.

During the dynamic simulation, the areal density of atoms in the depth intervals may be modified due to the deposition of projectiles, or due to relocation of recoil atoms. From experience, an average reasonable statistical quality is obtained if the relative change of the areal density per incident pseudoprojectile of atoms in any depth interval does not exceed a few percent of the initial areal density during the entire simulation run. By default, the program adjusts for the predefined total fluence and depth interval structure automatically in such a way that this criterion is approximately fulfilled.

Optionally, the user may enhance or deteriorate the statistical quality by means of a preset relative precision factor, which will increase or decrease the computation time, respectively,

Naturally, N_p^0 must be an integer number. For convenience, it is taken as a multiple of 10, 100, 1000 or 10000 by default.
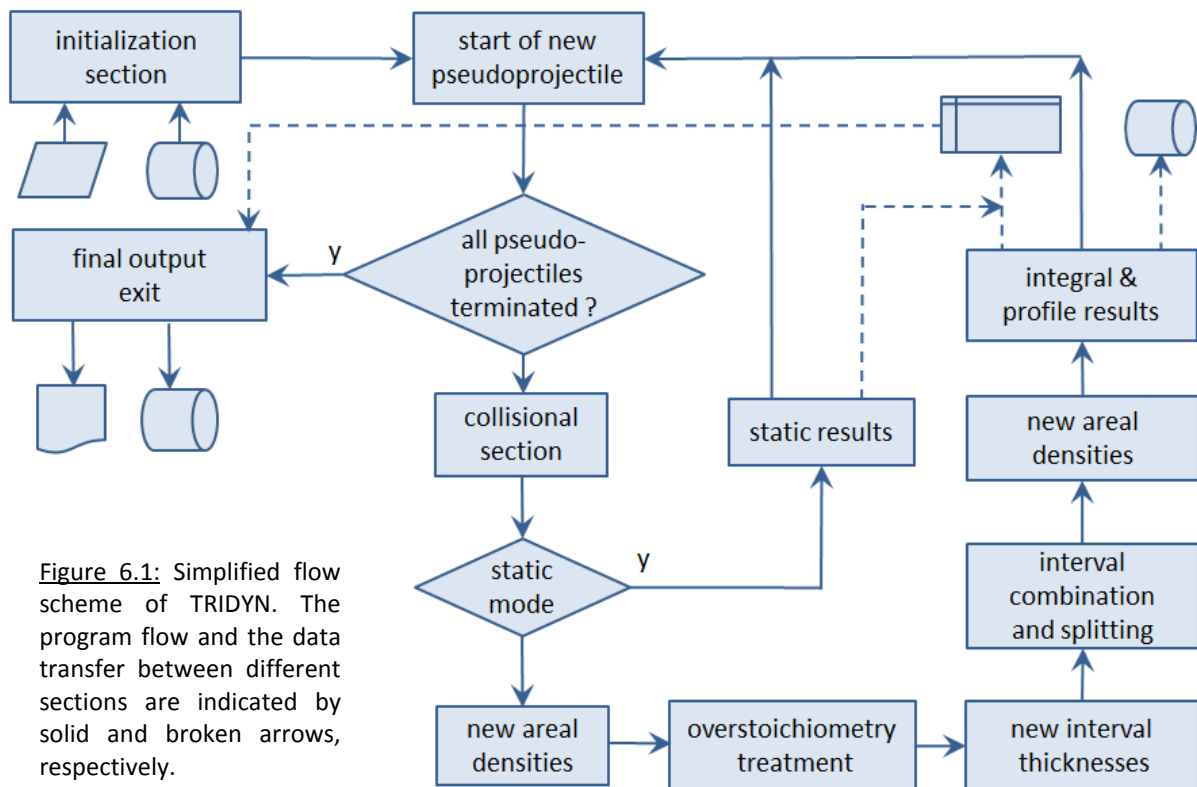
Figure 6.1: Simplified flow scheme of TRIDYN. The program flow and the data transfer between different sections are indicated by solid and broken arrows, respectively.

6. Basic flow of the simulation

Fig. 6.1 shows a simplified flow scheme of the program. Within the initialization section, the user input is processed for the definition of the program control parameters including the irradiation conditions, and the setup of the system and the local composition, so that the system becomes ready for the launch of the first pseudoprojectile.

The subsequent collisional section (see sect. 7 for details) launches one pseudoprojectile and processes the development and termination of the collision cascade, being represented by the pseudoprojectile and the generated primary and secondary pseudo recoil atoms. Slowed-down

pseudoprojectiles, sputtered pseudo recoil atoms as well as generated vacancies and interstitials are recorded for further processing.

The dynamic relaxation (see sect. 8 for details) of the system is accomplished in several subsequent steps of the treatment of overstoichiometry, the definition of new depth interval thicknesses, actions to address depth intervals with excessive gain or loss of material, and finally the setup of the local partial and total areal densities to be available for the subsequent collisional run. Intermediate integral data as function of the fluence (such as depth-integrated areal densities of the components or sputtering yields) are stored as well as compositional depth profiles, and, optionally damage profiles.

7. Collisional algorithms

The collisional section of TRIDYN is based on the well-established algorithms of TRIM, as, e.g., described in the book by Eckstein[10]. Therefore, only specific additions and modifications will be addressed to some detail. The algorithms work fully in three dimensions.
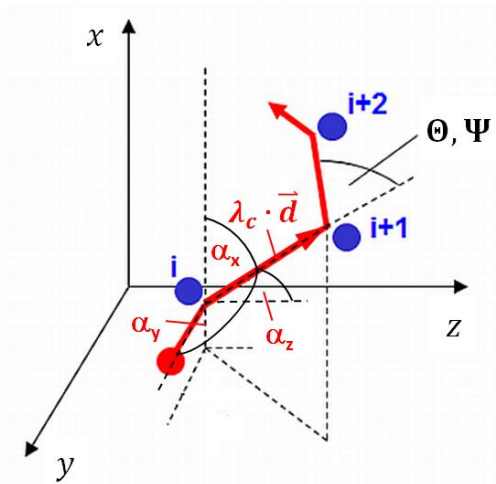
Figure 7.1: Moving atom trajectory between collisions with target atoms indexed as $i, i + 1, \ldots$ λ_c denotes the free pathlength, $\vec{d}$ the directional unity vector of motion, $\alpha_{x \ldots z}$ the directional angles, and Θ and Ψ the polar and azimuthal deflection angles, respectively.

7.1   Trajectories and collisions

The trajectories of pseudoatoms (projectiles or recoil atoms) in the solid body are described as a sequence of straight line segments between elastic collisions, which represent the asymptotic trajectories before and after each elastic collision (see Fig. 7.1). For the description of the atomic transport in an amorphous medium, a fixed free pathlength between the collisions is employed according to

$$\lambda_c = \bar{n}^{-1/3} \tag{7.1}$$

where $\bar{n}$ is the average total atomic density of the bulk at the beginning of the simulation. Following the "density conservation" concept of TRIM, one close collision per average atomic volume is modeled by choosing the collision target randomly within a circle of area $\pi p_{max}^2 = \bar{n}^{-2/3}$ (see Fig. 7.2), where p_{max} denotes the maximum impact parameter. Additional soft collisions (default: one) can be added[5] with impact parameters in annuli corresponding to one additional atomic volume each. The collisional algorithm accounts for the "time integrals" as shown in Fig. 7.2, and corrects the individual free pathlengths correspondingly in order to maintain density conservation.

Before each collision, the atomic species of target atom is randomly selected according to the local composition. With the impact parameter chosen in the above way, the related deflection angle Θ

and the recoil emission angle Φ are calculated by classical mechanics using a universal screened Coulomb scattering potential[11] given by

$$V(R) = \frac{Z_A Z_B e^2}{4\pi\varepsilon_0 R}\,\varphi_s\left(\frac{R}{a}\right)$$ (7.2)

where R denotes the distance between the collision partners, Z_A and Z_B their atomic numbers, φ_s the screening function in the "Kr-C" parametrization[12], and a the screening radius, for which the Firsov formulation[13]
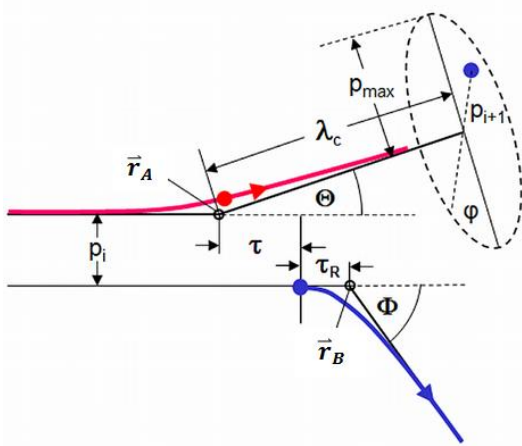

Figure 7.2: Details of an elastic collision with sequence no. i and position of the subsequent target atom in the laboratory system. The moving atom (A, red dot and trajectory) approaches the target atom (B, blue dot and trajectory) at an impact parameter p and becomes deflected by a polar angle Θ, while the recoil atom is launched under a polar angle Φ. The asymptotic trajectories are displaced from the site of collision by the so-called time integrals τ and τ_R. The position of the subsequent target atom is chosen by random selection of the subsequent impact parameter and the azimuthal angle φ. φ determines also the azimuthal deflection angle Ψ (see Fig. 7.1) and the azimuthal recoil emission angle (not shown) of the subsequent collision.

$$a_F = \frac{0.8853\, a_0}{\left(\sqrt{Z_A} + \sqrt{Z_B}\right)^{2/3}}$$ (7.3)

is selected, with a_0 denoting the first Bohr radius. The scattering function $\Theta(p)$ is calculated using the "magic" approximation proposed by Biersack and Haggmark[2].

The elastic (or "nuclear") energy loss of the moving atom, which is equal to the kinetic energy transfer T to the target atom, is directly related to the deflection angle Θ. The inelastic or electronic energy loss resulting from the interaction with the target electrons can be chosen to act nonlocally along the free path according to the Lindhard-Scharff formula[14], or locally in dependence on the impact parameter according to Oen and Robinson[15]. The former limits the regime of kinetic energies E in the simulation to $E < 25\ keV/amu$. As default setting, TRIDYN uses an equipartition of local and nonlocal electronic energy loss.

The initial kinetic energy of a new pseudo recoil atom generated during the collision is given by

$$E_0 = T - U_b$$ (7.4)

with the "bulk binding" energy U_b, with the default setting[10] $U_b = 0$.

All pseudoatoms are traced until their kinetic energy falls below a predefined, species-specific cutoff energy U_{co}, or until they leave the boundaries of the computational volume. By default, the cutoff energy of all species is adjusted to the lowest elemental surface binding energy occuring in the system. Following this, the pseudoatoms are registered as deposited, scattered or transmitted projectiles, or as sputtered or transmitted recoil atoms.

7.2 Solid – vacuum transitions

For the incident pseudoprojectiles, or when a pseudoatom travelling in the bulk arrives in vacuum above or below a surface (the top surface or the bottom surface in case of a free-supported film), a surface transition routine is entered which makes use of the standard planar potential barrier model of the surface[16]. Depending on the actual energy of the pseudoatom, the direction of motion with respect to the surface and the local surface binding energy U_s, the pseudoatom is either transmitted through the surface with its trajectory being deflected, or it may be backreflected at the surface in case of a solid-to-vacuum transition.

The actual surface binding energy is calculated from the actual composition of the surface layer

$$U_s = \sum_{j=1}^{N_c} q_j U_{i,j}$$
(7.5)

where i denotes the atomic species of the moving pseudoatom, and $U_{i,j}(i,j = 1 \dots N_c)$ represent the surface binding matrix elements which describe the interaction of the component i with the component j. The elements of the matrix, which is normally symmetric, can be derived from the surface binding energy of the pure components, $U_{s,i}$, which vary from about 2 eV to about 8 eV for solid materials. A simple choice (default in TRIDYN) is

$$U_{i,j} = \begin{cases} 0 & \text{if } i \text{ or } j \text{ represents a gaseous component} \\ \dfrac{U_{s,i} + U_{s,j}}{2} & \text{if } i \text{ and } j \text{ represent solid components} \end{cases}$$
(7.6)

Optionally, surface binding energy matrix elements for selected compounds may be taken from the internal list of compounds (see sect. 3 and Appendix D). A detailed recipe for the definition of the matrix elements is given in Appendix A.

7.3 Recoil generation, vacancy and interstitial formation

As described in sect. 7.1, new pseudo recoil atoms are generated by the elastic collisions. These may either become sputtered from the body or displaced within the body, leaving a pseudo vacancy at the original position, and a pseudo interstitial atom at the new position. Recoil atoms can only be displaced if their initial energy exceeds the displacement threshold energy U_d. Conventionally, the displacement threshold is defined for an isolated displacement in an otherwise perfect crystalline solid, with values ranging from about 10 eV to about 80 eV for solid materials. With the typical fluences applied for ion-induced modification of a material at limited temperature, the material may become quickly heavily damaged or even amorphized, so that a lower initial recoil energy may be sufficient to obtain a stable displacement. From experience with numerous systems and in comparison to experiments, a universal default value of $U_d = 8$ eV is recommended, which is consistent with the value proposed by Sigmund and Gras-Marti[17] for ion-induced atomic mixing.

Thus, the program generates a pseudo vacancy in a depth interval where an over-threshold pseudo recoil atom is generated, and a pseudo interstitial atom where an over-threshold pseudo recoil atom comes to rest. Additional pseudo interstitials result from the slowing-down of incident pseudoprojectiles. Subthreshold recoil atoms have to be considered in the simulation on order to correctly model sputtering with its low surface binding energies. Consequently, a sputtered sub-threshold recoil atom leaves a vacancy behind in the depth interval of its origin.

Pseudoatoms arriving at the bottom boundary of a semi-infinite body are discarded in the simulation. They may leave behind an unrealistically high number of vacancies close to the bottom boundary and thus result in an unrealistic shrinking of the structure. Consequently, such vacancies

are artificially removed by re-inserting the recoil atom into the depth interval of origin. This, however, induces artifacts in the defect distribution, which, however, might be tolerated in regions of less interest. Otherwise, x_{max} should be chosen large enough so that only a small or zero fraction of generated pseudo recoil atoms arrives at the bottom boundary.

7.4   Damage recording

A one-dimensional profile of ion-induced point defect damage is optionally **r**ecorded during the collisional run by counting the areal density of generated vacancies and relating it to the total areal density in that depth interval, so that the relative number of generated vacancies, measured in dpa (displacements per atom) is obtained. At increasing fluence, this number increases steadily. In reality, any solid will only accommodate a certain fraction of point defects. Therefore, the option of saturable damage is included. Then, if a pseudovacancy is generated, the increase of the fraction of vacancies q_v in the respective depth interval with areal density v is modelled as

$$\Delta q_v = \frac{\psi_0}{v}(q_v^{max} - q_v) \tag{7.7}$$

which limits the damage to a predefined level q_v^{max} (normally, $q_v^{max} \leq 1$ will be chosen, with $q_v^{max} = 1$ limiting the damage to 1 dpa).

7.5   Dynamic updating of local areal densities

As a new feature in TRIDYN_2017, the local partial and total areal densities are dynamically updated already during the collisional phase, according to the removal or deposition of pseudoatoms in the respective depth intervals (see sect. 7.3). In this way, a specific pseudoatom cannot be removed twice from its depth interval. This may result in low partial areal densities of the constituents, so that only fractions of a pseudoatom may remain. If the respective constituent is selected for another recoil generation, the program zeroes the respective partial areal density, and treats the resulting recoil atom as a partial pseudoatom for areal density conservation. In addition, the collision probability in depth intervals with dynamically diminished areal density is randomly reduced.

8.   Dynamic relaxation

8.1   Treatment of overstoichiometry

The user may define an overall maximum atomic fraction q^{max} for any of the components of the system, e.g. in order to limit the local composition to the stoichiometry of a compound, or to discard any slowed-down rare-gas projectiles. There are three options:

(i)   Direct reemission: The fraction of the local partial areal density of a component l, which results in an atomic fraction exceeding q_l^{max}, is removed from the system directly after the deposition of a pseudoprojectile or a pseudo recoil atom, resulting in an atomic fraction of q_l^{max}. The excess adds to the reemitted amount of the species l. This option is recommended when the retention of an incident projectile species shall be limited, or this species shall be completely discarded by setting, $q^{max} = 0$, such as for rare gas implantation.

(ii)   Saturable deposition: This option is similar to (ii), with however, a gradual approach of the local atomic fraction to the preset maximum. With the local atomic fraction q_l before the deposition of a new pseudoprojectile or pseudo recoil atom, the additional areal density to be inserted is taken as

$$\Delta_l = \psi_0 \left(1 - \frac{q_l}{q_l^{max}} \right) \tag{8.1}$$

whereas the remaining areal density transported by the newly deposited pseudoatom, $\psi_0(1 - \Delta_l)$, is added to the reemitted amount of component l. This option is in particular adequate for the deposition of slow incident atoms (such as for the modelling of ion-assisted deposition), where it mimics a saturable chemisorption of the incident species.

(iii) <u>"Diffusive" release</u>: When applied to the limitation of the stoichiometry of a certain compound in the bulk, option (i) of (ii) may result in an artificial excessive loss of the species with $q^{max} < 1$, as in reality the excess amount might diffuse to a neighboring site which is still understoichiometric, and be inserted there. This is modelled by the transfer of the local excess areal density to the closest depth interval which is still understoichiometric. If such an interval cannot be found, i.e. if the entire bulk is saturated, the excess amount is added to the reemitted amount.

8.2   New depth interval spacings and areal densities

With the new local areal densities resulting from the collisional and algorithms and overstoichiometry treatment (if activated), the thicknesses of the altered depth intervals are adjusted according to eq. (3.3). If the resulting thickness of any depth interval exceeds $1{,}5\Delta x$, the interval is split into two intervals of equal thickness. If the thickness falls below $0{,}5\Delta x$, the interval is combined with the neighbor interval at larger depth. Correspondingly, one depth interval is added or removed, respectively, to or from the bottom of the computational volume. In case of interval combination, the added interval of thickness Δx_0 is empty in case of a free-supported thin film geometry, or it carries the composition of the initial bottom interval in case of a semi-infinite medium. As a result, the bottom depth and/or the thin film thickness may vary in the course of the dynamic relaxation.

Dynamic integral data and compositional and damage (if activated) depth profiles are finally calculated after preset increments of the number of incident pseudoprojectiles. The output depth profiles are defined on the initially equidistant layer structure with N_x spacings of thickness Δx_0, which is obtained by interpolation of the dynamic internal non-equidistant structure.

9. Static operation

Although TRIDYN is basically set up for ion and recoil atom tracing in connection with dynamic relaxation of the material, it can optionally be operated in static mode. Then, the program acts as a layer-based BCA simulation of the TRIM[4] type, where each new incident projectile finds the same unmodified target structure.

The predefined fluence ϕ_0 (still denoting the number of incident projectiles per unit area for the run) determines merely the statistical quality of the results. (As the code uses the algorithms of sect. 5 also in static operation, the statistical quality can also be adjusted by the precision parameter π_0.)

In static mode, the relaxation sections (see Fig. 6.1) are fully skipped. In contrast to absolute local atomic densities and compositions versus projectile fluence being delivered by the dynamic operation, the results of static operation have to be understood as density and composition changes of the initial structure per increment of fluence.

References

[1] M.T. Robinson, O.S. Oen, The Channeling of Energetic Atoms in Crystal Lattices, Appl Phys Lett, 2 (1963) 30-32.

[2] J.P. Biersack, L.G. Haggmark, A Monte-Carlo Computer-Program for the Transport of Energetic Ions in Amorphous Targets, Nucl Instrum Methods, 174 (1980) 257-269.

[3] J.F. Ziegler, M.D. Ziegler, J.P. Biersack, SRIM - The stopping and range of ions in matter (2010), Nucl Instrum Meth B, 268 (2010) 1818-1823.

[4] J.F. Ziegler, Particle interactions with matter. http://www.srim.org (2011).

[5] J.P. Biersack, W. Eckstein, Sputtering Studies with the Monte-Carlo Program Trim.Sp, Appl Phys a-Mater, 34 (1984) 73-94.

[6] W. Moller, W. Eckstein, Tridyn - a Trim Simulation Code Including Dynamic Composition Changes, Nucl Instrum Meth B, 2 (1984) 814-818.

[7] W. Moller, W. Eckstein, J.P. Biersack, Tridyn - Binary Collision Simulation of Atomic-Collisions and Dynamic Composition Changes in Solids, Comput Phys Commun, 51 (1988) 355-368.

[8] A.S. Mutzke, R., SDTrimSP-2D: Simulation of Particles Bombardment on a Two Dimensional Target, Max-Planck-Institut für Plasmaphysik, Report IPP 12/4, 2009.

[9] W. Moller, TRI3DYN-Collisional computer simulation of the dynamic evolution of 3-dimensional nanostructures under ion irradiation, Nucl Instrum Meth B, 322 (2014) 23-33.

[10] W. Eckstein, Computer simulation of ion-solid interactions, Springer, Berlin, 1991.

[11] J. Lindhard, V. Nielsen, M. Scharff, Approximation Method in Classical Scattering by Screened Coulomb Fields (Notes on atomic collisions, I), Matematisk-fysiske meddelelser 36,10; Det Kongelige Danske Videnskabernes Selskab, København, 1968.

[12] W.D. Wilson, L.G. Haggmark, J.P. Biersack, Calculations of Nuclear Stopping, Ranges, and Straggling in Low-Energy Region, Phys Rev B, 15 (1977) 2458-2468.

[13] N. Bohr, J. Lindhard, Electron Capture and Loss by Heavy Ions Penetrating through Matter, Mat Fys Medd Dan Vid, 28 (1954) 1-U30.

[14] J. Lindhard, M. Scharff, Energy Dissipation by Ions in the keV Region, Phys Rev, 124 (1961) 128-130.

[15] O.S. Oen, M.T. Robinson, Computer Studies of Reflection of Light-Ions from Solids, Nucl Instrum Methods, 132 (1976) 647-653.

[16] P. Sigmund, Theory of Sputtering I. Sputtering Yield of Amorphous and Polycrystalline Targets, Phys Rev, 184 (1969) 383-416.

[17] P. Sigmund, A. Grasmarti, Theoretical Aspects of Atomic Mixing by Ion-Beams, Nucl Instrum Methods, 182 (1981) 25-41.

INPUT DATA

The input data stream of TRIDYN consists of a set of control parameters and additional input files, which are required in case of special options which will be described below.

With each description of an input record (grey/blue fields below), an example will be given (red fields where applicable) for a layered substrate of 9 nm SiO_2 on Si, which is simultaneously exposed to energetic Ne ion irradiation at an energy of 20 keV and a fixed angle of incidence of 60°, and to a thermal flux of Si atoms with a gas-kinetic cosine angular distribution. The ion-to-neutral ratio is Ne:Si = 1:4, and the total fluence of impinging atoms is 10^{17} cm^{-2}. The incorporation of Ne is suppressed.

Control parameters (arbitrary filename)

The control parameter data set consists of subsequent records in the following sequence:

1st record:

10-character arbitrary run ID *run_id_abc* (columns 1-10) plus arbitrary comment
SiO_NeSi00   20 keV, 60° Ne + therm. Si -> SiO2/Si

followed by a set of obligatory control records and a set of optional control records. Both consist of a 4-character identifier plus a number of specific parameters, all individual data being separated by blanks. Records headed by # are skipped and may be used for comments. A blank line or the end of the data set terminates the control parameter input.

Obligatory control parameters

The obligatory control records must be grouped in the following order with the following contents:

2nd record: general control data

identifier	mode	total fluence of irradiaton $(Å^{-2})$	initial compositional profile option
'cdat'	idrel = 0: dynamic < 0: static	flct > 0	iq0 = 0: homogeneous < 0: from layer input
cdat 0 10. -1			

The total fluence is defined as sum of the partial fluences for the individual irradiation conditions (see below).

3rd record: geometry

identifier	bottom boundary(Å)	nr. of depth intervals	system

'geom'	xmax	nqx	dthf = 0: semi-infinite body
			     > 0: free-supported thin film with thickness
			         from depth node closest to dthf
			     < 0: free-supported thin film with thickness from
			         empty layers in layer input

geom 600. 200 0			

The input determines the initial depth spacing dqx=xmax/nqx, which should be larger than the collisional free pathlength (typically around 3 Å).
The maximum numbers of depth intervals is nqx =5000.

4th record: atomic data of the components

identifier	chemical symbols
'atda'	up to 10 max.-2-character chemical symbols of the components
atda Ne Si O	

any symbol may occur more than once (e.g., to assign different atomic masses or densities);
the total nr. of entries defines ncp = nr. of components, the sequence determines the component id no.s nocp

additional record (only if iq0 = 0):   initial atomic fractions

identifier	atomic fractions
'comp'	qu0(1..ncp) in order given by 'atda' (must add to 1)

final obligatory record(s):   irradiation parameters (one record for each irradiation condition)

identifier	component id no.	energy of incidence (eV)	angle of incidence (°)	fraction of total irradiation
'irra'	icp	e0	alpha	qubeam (fractions must add to 1)
irra 1 20000. 60.				0.2
irra 2 0. 0.				0.8

the sequence of the records determines the id no.s noir of the irradiation conditions;
alpha is the angle of incidence with respect to the x (in-depth) direction; the plane of incidence is the x-y plane

Optional control parameters (frequently applied)

The optional control records may be arranged in arbitrary order. The same option may be applied repeatedly; the last occurrence will overwrite previously defined data.

The most frequently occurring options will be listed first. Where applicable, default values will be listed which the program uses without optional control.

precision of dynamic alteration

identifier	relative precision parameter
'prec'	prcs default 1.

a lower precision parameter improves the statistical quality of the results
see sects. 5 and 8 for details

compound data

identifier	chemical symbol of compound
'cmpd'	cmpid (max. 6 characters)
cmpd	SiO2

from an internal list of frequently used compounds (see Appendix D), atomic density and surface binding energy data are automatically inserted
if several compound with identical second element are defined (e.g., TiO_2 and SiO_2), the more prominent one should be defined last; if needed, density and surface binding parameters can be adjusted using the 'dens' and 'sbei' options, respectively (see below)
option works for max. 2 entries of the same element in the component list (see 'atda' above)

excess stoichiometry treatment (not active in static mode)

identifier	component ID	max. atomic fraction	action switch

'exst'	nocp	qumax
		0 <=
		qumax
		< 1
		default 1
			ires
			= 1: direct reemission if atomic fraction exceeds qumax
			= 2: incorporation of fraction (1-qu/qumax),
			        reemission of fraction qu/qumax
			= 3: "diffusive" transfer to nearest unsaturated
			        depth interval

exst	1	0.	1
exst	3	0.6667	3

useful if overstoichiometry of a specific compound shall be suppressed, or if incorporation of a specific projectile species shall be limited
qu denotes the actual atomic fraction in the respective depth interval

displacement threshold

identifier	component ID	displacement threshold energy (eV)
'edsp'	nocp	ed default 8 eV

the number of generated vacancies and interstitials increases at decreasing displacement threshold; the conventional (higher) values for pure crystalline solids are not appropriate in general; however, specific data may be employed if better knowledge is available

<u>fixed nr. of pseudoprojectiles</u>

identifier	nr. of pseudoprojectiles
'pspr'	nh

By default, the total number of pseudoprojectiles of the run is calculated from the total fluence (see 'cdat' above) and the predefined precision parameter (see 'prec' below). Alternatively, the user may predefine the total number of pseudoprojectiles (the predefined precision parameter is then ignored). This may option may be preferable for a static run (see 'cdat' above), or for initial testing of a dynamic run with a small number of pseudoprojectiles

<u>output frequencies</u>

identifier	frequency of log messages	frequency of integral outputs	frequency of 3D profile outputs

'outf'	idfout
	nr. of performance log messages during entire run
	=1,2,5,10,20,50,100,
	  200,500
	=0: output suppressed
	default 100
		iddout
		nr. of integral data outputs during entire run
		=1,2,5,10,20,50,100,
		  200,500
		=0: output suppressed
		default 50
		(ignored in static mode)
			idqout
			nr. of 3D profile outputs during entire run
			=1,2,5,10,20,50,100,
			  200,500
			=0: output suppressed
			default 10
			(ignored in static mode)

outf 50 100 10			

at low fluence and correspondingly low number of projectiles, the frequencies are automatically reduced if applicable

<u>damage profile calculation</u>

identifier	max. damage level (dpa)
'damg'	dmg0 = 0: vacancy generation unlimited > 0: vacancy generation limited to dmg0 (dynamic mode only)

dynamic mode: periodic output of damage profile together with compositional profile data outputs (see idqout above)
static mode: final output of average damage generation per unit of fluence

<u>surface composition: integration depth</u>

identifier	integration depth (Å)
'dsrf'	dsf default: 10

for the generation of surface composition data; e.g., for the comparison to experimental results from diagnostics with differerent depths of analysis

Optional control parameters (less frequently applied)

distributed angles of incidence

identifier	irradiation condition ID	type of angular distribution	parameter 1	parameter 1	parameter 3
'angd'	noir	iadis = 1: 2D axially symmetric Gaussian = 2: 2D axially symmetric cosine^x default 0	adpar1 iadis = 1: fwhm (°) iadis = 2: fwhm (°) (standard gas-kinetic cosine[1] distribution requires fwhm=120°)	adpar2 iadis = 1: cutoff angle in units of std. deviation iadis = 2: exponent x	adpar3 ignored (reserved for later additions)
angd 2 2 120. 1. 0.					

see Appendix B for a detailed description of the available beam angular distributions

special irradiation options

identifier	irradiation condition ID	incident energy scheme	final ramp energy (eV)
'irrd'	noir	ie0 < 0: randomly from predefined energy distribution > 0: linear energy ramp (e0 is start energy) =0: default	e0f (ignored if ie0 <= 0)

collisional parameters

identifier	max. order of weak collision shells	recoil on/off switch	recoil suppression range
'coll'	iwc default 1	iproj < 0: treatment of incident projectiles only default 0 (treatment of all atoms)	jsp1,jsp2 suppression of recoils with cpt. ID's jsp1…jsp2 default 0,0: all recoils treated

single surface binding energy matrix element

identifier	component ID 1	component ID 2	surface binding energy (eV)
'sbei'	nocp1 line no. of SBE matrix	nocp2 column no. of SBE matrix	sbe$_{nocp1,nocp2}$ default from internal list or from compound option

e.g., to allow for an asymmetric SBE matrix
simplified recipes for the definition of surface binding energies are found in Appendix A
make sure to position 'sbei' after 'cmpd' if applicable, as the latter might overwrite the desired value

complete surface binding energy matrix

identifier	
'sbem'	(none) default from internal list or from compound option

ncp additional records: lines of surface binding energy matrix

$sbe_{1,1} \dots sbe_{1,ncp}$
……
$sbe_{ncp,1} \dots sbe_{ncp,ncp}$

the surface binding energy matrix is usually, but need not be, symmetric
simplified recipes for the definition of surface binding energies are found in Appendix A

binary compound surface binding model

identifier	binary compound SBE identifier
'sbec'	csbe = x>0: discrete variation of SBE in a cpt. no.2 - cpt . no.3(x) compound = 0 (default) continuous variation according to standard SBE matrix

a sub-stoichiometric compound shows often a phase separation of the stoichiometric compound and the excess pure element. Then, the surface binding energy of the excess element varies discretely and is randomly selected according to the actual local surface composition. This model is implemented for a binary compound consisting of component 2 and component 3, with component 2 representing the excess element. Example: SiO_x => SiO_2+Si; component 2 = Si; component 3 = O; csbe = 2

specific atomic mass

identifier	component ID	atomic mass (amu)
'mass'	nocp	am default from internal list

elemental masses may be changed, e.g., for treating different isotopes

specific bulk binding energy

identifier	component ID	binding energy (eV)
'eblk'	nocp	be default 0

should only be activated for special test applications

cutoff energy

identifier	component ID	cutoff energy (eV)
'efin'	nocp	ef default calculated from min. surface binding energy

cutoff energies may be enlarged to decrease the computation time when the latter is dominated by the collisional processes. Increasing the cutoff energies above surface binding energies or damage thresholds, respectively, will reduce sputtering and defect formation

specific electronic stopping correction factor

identifier	component ID	correction factor
'elsc'	nocp	ck default 1.

elemental low-energy stopping data, which are more precise than the ones calculated from universal formulas, can, e.g., be obtained by fitting to specific data calculated using SRIM

electronic stopping mode

identifier	mode switch
'elst'	inel =1: nonlocal =2: local =3: (default) equipartitioned local/nonlocal

nonlocal electronic stopping may be preferable for light projectiles of relatively high energy

specific atomic density

identifier	component ID	atomic density (Å^{-3})
'dens'	nocp	dns0 default from internal list or from compound option

specific atomic densities may be defined, e.g., for a specific compound which is not listed internally, or for rare gas incorporation which shall not contribute to volume expansion (large values)
make sure to position 'dens' after 'cmpd' if applicable, as the latter might overwrite the desired value

depth limitation of profile outputs

identifier	depth interval range
'outl'	nqxn,nqxx 1 < nqxn < nqxx < nqx

in cases where, e.g., the depth extension is defined by the size of the collision cascade, but significant modifications of the body occur only in a certain regime of the body, the outputs may be spatially limited to reduce the output file size

pseudoprojectile list mode outputs

identifier	pseudoprojectile ranges and scattering	pseudo recoil atom sputtering and displacements
'outs'	irgl,ibsl irgl > 0: deposited pseudoprojectiles ibsl > 0: backscattered/transmitted pseudoprojectiles default 0,0	ispl,ircl ispl > 0: sputtered pseudo recoil atoms ircl > 0: deposited pseudo recoil atoms default 0,0
outs 1 0 1 0		

Particularly useful in static mode (idrel=0) to generate pseudo atom statistics .In dynamic mode, outputs are generated for the entire run. However, from the included pseudoprojectile sequence no.s, fluence-dependent subsets can be extracted.

deposited energy profiles

identifier	
'edep'	(none)

generates 1D deposition profiles of energy deposited into nuclear and electronic collisions, averaged over the entire run

initial random seed

identifier	random seed no.
'rand'	irand default 12345

Additional input files

1D compositional profile (if iq0 < 0)

filename	atomic fractions of components
run_id_abc.lay	nqx records with increasing ix = 1...nqx, each containing ncp data qu0(jp): initial atomic fractions of cpts. 1...ncp for each depth interval, qu0(jp) must either add to 1 or all vanish

distribution of energy of incidence (if ie0 < 0)

filename	energy distribution function
run_id_abc.ed*n* *n* denoting the irradiation condition ID no.	e (eV), f(e) max. 1000 data pairs in subsequent records energy spacing must be equidistant f(e) will be normalized automatically

OUTPUT DATA

Initial parameter protocol

List of input parameters from default settings, user input, and derived parameters; for, e.g., later processing of the simulation results.

(Data are listed in the following sequence of records)

filename		*run_id_abc_*indat.dat				
run ID						
flct	pseu	prcs	nh	ncp	nirr	idrel
total fluence (Å^{-2})	nr. of real atoms per pseudoatom	relative precision parameter	nr. of pseudo-projectiles	nr. of elemental components	nr. of irradiation conditions	operation mode switch
iproj		irand				
pseudoprojectile-only switch		initial random seed no		.		
xmax		nqx		dthf		dsf
x extensions of the computational volume (Å)		nr. of depth intervals		thickness of free-supported thin film (Å)		surface composition integration depth (Å)
inel, iwc		dmg0	csbe	jsp1,jsp2		
electronic stopping and weak collision switches		max. damage level (dpa)	stoichiometry special surf. binding model	recoil atom suppression switches		
ifout, idout, iqout			nqxn,nqxx			
log, integral and compositional and damage profile output frequencies			profile output depth interval range			
irgl,ibsl,ispl			ispl,ircl			
list mode output switches projectile range and scattering			list mode output switches recoil sputtering and deposition			

ncp groups	zz,m	be,ef,ed		qu	dns0	ck
	atomic number and mass	bulk binding, cutoff and displacement threshold energies (eV)		initial atomic fraction	component atomic density (Å^{-3})	electronic stopping correction
	ires		qumax		sbv	
	overstoichiometry treatment switch		composition limit		surface binding energy matrix elements (eV) (1…ncp)	

nirr groups	ircp	ie0,e0,e0f	alpha0	qubeam	iadis, adpar (1…3)
	component ID	incident energy scheme switch, start energy (eV), final energy (eV)	irradiation angle (°)	beam fraction	angular distribution switch, parameters

Dynamic mode outputs (in the following, the listed output data fill one record each)

Integral data

(frequency determined by iddout)

areal densities of components

filename	fluence (Å^{-2})	areal densities (Å^{-2})
*run_id_abc*_ardn.dat	flc	ard (1…ncp)

surface composition

filename	fluence (Å^{-2})	surface atomic fractions
*run_id_abc*_disp.dat	flc	qus (1…ncp)

for the surface integration depth, see option 'dsrf' above

reemitted amounts of components

filename	fluence (Å^{-2})	reemitted amounts (Å^{-2})
*run_id_abc*_reem.dat	flc	reem (1…ncp)

reemitted amounts, being calculated if ires > 0 for the respective component

sputtering yields of components

filename	fluence (Å^{-2})	sputtering yields
*run_id_abc*_spyl.dat	flc	spyd (1…ncp)

the sputtering yields are related to the total number of incident projectiles (all irradiation conditions)

surface recession (for semi-infinite medium only)

filename	fluence (Å^{-2})	surface recession (Å)
*run_id_abc*_srrs.dat	flc	srrc > 0: surface recession by sputtering < 0: surface extension by deposition or swelling

film thickness (for free-supported thin film only)

filename	fluence (Å^{-2})	film thickness (Å)
*run_id_abc*_thtf.dat	flc	thif

areal densities of vacancies

filename	fluence (Å^{-2})	areal densities (Å^{-2})
*run_id_abc*_disp.dat	flc	ardd (1…ncp)

Profiles

(frequency determined by idqout)

<u>compositional profiles</u>

filenames	compositional profile
*run_id_abc*_pr*nnn*.dat *nnn* denoting the sequence no. of the profile output	nqx records with increasing ix = 1...nqx, each containing x: mean depth of depth interval (Å) dns: total atomic density (Å^{-3}) qu(1...ncp): elemental atomic fractions

<u>vacancy profiles (if damage calculation option activated)</u>

filenames	vacancy distribution
*run_id_abc*_vg*nnn*.dat *nnn* denoting the sequence no. of the profile output	nqx records with increasing ix = 1...nqx, each containing x: mean depth of depth interval (Å) dam(1...ncp): damage level (dpa)

Static mode outputs

<u>initial areal densities of components</u> (one record only)

filename	fluence (Å^{-2})	areal densities (Å^{-2})
*run_id_abc*_ardn.dat	flc = 0	ard (1...ncp)

<u>initial surface composition</u> (one record only)

filename	fluence (Å^{-2})	surface atomic fractions
*run_id_abc*_srfc.dat	flc = 0	qus (1...ncp)

for the surface integration depth, see option 'dsrf' above

<u>static damage profile</u>

filename	vacancies per depth interval and increment of fluence (dpa Å)
*run_id_abc*_dpstc.dat	nqx records with increasing ix = 1...nqx, each containing x: mean depth of depth interval (Å) dam(1...ncp): local damage created by displacements of species 1...ncp per increment of fluence

static single relocation profile

filename	nr. of atomic relocations per depth interval and increment of fluence (Å)
*run_id_abc_*prstc.dat	nqx records with increasing ix = 1...nqx, each containing x: mean depth of depth interval (Å) del(1...ncp): average local gain (>0) or loss (<0) of atoms of species 1...ncp per depth interval and increment of fluence

Pseudoatom list mode outputs

one record per event as listed below
In dynamic mode, each list mode output record reflects the momentary state of the system. This implies that the x scale might fluctuate even within only a few subsequent records, which is due to the dynamic adjustment of the depth intervals. To obtain pseudoprojectile statistics at a predefined fluence without this fluctuation, it is recommended to perform a subsequent static simulation with the compositional profile output of the original run at the desired fluence as the starting profile – see "Additional input files" above

deposited pseudoprojectiles (if irgl>0)

filename	fluence (Å^{-2})	component ID no.	deposition site coordinates (Å)
*run_id_abc_*rglst.dat	flc	nocp	x,y,z

scattered pseudoprojectiles (if ibsl>0)

filename	fluence (Å^{-2})	component ID no.	energy (eV)	directional cosines	emission site coordinates (Å)
*run_id_abc_*bslst.dat	flc	nocp	e	cx,cy,cz	x,y,z

sputtered pseudo recoil atoms (if ispl>0)

filename	fluence (Å^{-2})	component ID no.	energy (eV)	directional cosines	emission site coordinates (Å)
*run_id_abc_*splst.dat	flc	nocp	e	cx,cy,cz	x,y,z
	start energy (eV)	start site coordinates (Å)			
	es	xs,ys,zs			

deposited pseudo recoil atoms (if ircl>0)

filename	fluence (Å^{-2})	compo-nent ID no.	deposition site coordinates (Å)	start energy (eV)	start site coordinates (Å)
*run_id_abc*_rclst.dat	flc	nocp	x,y,z	es	xs,ys,zs

Nuclear and electronic energy deposition profiles (if option activated)

filenames	energy density deposited into nuclear or electronic collisions
*run_id_abc*_ed3dn.dat, *run_id_abc*_ed3de.dat,	nqx records with increasing ix = 1...nqx, each containing x: mean depth of depth interval (Å) edep (jp=1...ncp): average deposited energy by species 1...jp per incident projectile and depth interval (eV/Å)

Protocol output

filename
*run_id_abc*_out.dat

records all input data and provides global results such as pseudoatom statistics and atomic balances

Appendix A:

Collisional input parameters – hints and formulas

A1 Computational volume

The choice of the computational depth ($0...x_{max}$) is arbitrary to a large extent. For the semi-infinite body, it should normally be large enough to contain the entire collision cascade as it might be checked, e.g., by a TRIM simulation). However, there might be regions of less interest (such as at the bottom of the structure), so that the body might be cut there. However, this might cause artifacts (see sect. 7.3 above).

A2 Energy Parameters

As a BCA simulation, TRIDYN employs a diatomic interaction potential which is only repulsive. Therefore, in contrast to classical dynamics simulations, additional "solid state" energy parameters have to be defined.

As a general remark, the energy parameters should not be misused as fitting parameters, e.g. in order to reproduce experimental values. They should rather be chosen according to the best knowledge and according to TRIM and TRIDYN conventions and experience, as described in the following.

A2.1 Cutoff Energy

The cutoff energies of the different components, ef_i, set the energies at which any pseudoatom (projectile or recoil in the collision cascade) is stopped. Obviously, very long computation times result from very low cutoff energies, so that these should be chosen as high as possible. The upper limits depend on the problem itself. If only the slowing down and backscattering of projectiles is considered, rather high cutoff energies can be chosen, being only limited by the artificial range shortening at too high cutoff energy. In general, the choice of the cutoff energies must be consistent with the characteristic energies of the governing processes. For example, if sputtering is to be treated correctly, the cutoff energies of the target components should be equal or less than the surface binding energies sbe_i (see below). In order to further reduce the computation time for certain problems, it may be adequate to increase the cutoff energy of a projectile according to the energy transfer to the target atoms, resulting in

$$ef_{proj} = \frac{(m_{proj} + m_{target})}{4 m_{proj} m_{target}} sbe_{target}^{min} \tag{A1}$$

where sbe_{target}^{min} denotes the minimum of the occuring nonzero surface binding energies.

Note! In general, it is not justified to identify the cutoff energies with the displacement threshold energies (see A2.4) which are in the order of several 10 eV. This would reduce the computing time significantly, but suppress all cascade development below these energies, and thus, e.g., result in a significant underestimation of sputtering.

A2.2 Bulk Binding Energy

In a BCA simulation, the bulk binding energy, be_i, is subtracted from the energy transfer to the recoil atom before it is set in motion. A well-defined value for this energy is difficult to obtain. Therefore, it is often simply set to zero, with good results, e.g., for sputtering yields if other standard parameters are chosen as described here. It is also known from TRIM experience that an increase of the bulk binding energies to up to a few eV requires a corresponding decrease of the surface binding energies in order to obtain the same sputtering yields. It is recommended to set the bulk binding energies to

the default value of zero.

A2.3 Surface Binding Energy

The surface binding energies determine critically the sputtering yields. Theoretically, the sputtering yield is proportional to the inverse of the surface binding energy. The effective surface binding energy of each target component can be chosen in dependence on the actual surface composition. There are two different models.

In the standard approach ("**continuous variation**" of the surface binding energy), the surface binding energy of a surface atom i can be described as a linear combination of the surface atomic fractions, q_j, of all components j ($1 \leq j \leq ncp$, $\Sigma c_j = 1$). This assumes pairwise binary interaction of the surface atoms, being described by matrix elements sbv_{ij}, so that

$$sbe_i = \sum_{j=1}^{ncp} sbv_{ij} q_j \qquad \text{(A2)}$$

Eq. (A2) includes the simple choice of surface binding energies which are independent of the surface composition, by the default setting $sbv_{ij} = sbe_i$ for all components j.

Alternatively, the surface might decompose into different phases at a given composition, as, e.g., into a metal phase and a stoichiometric oxide phase in case of a substoichiometric oxide. This can be modeled by a "**discrete variation**" of the surface binding energy, where the surface composition determines the probability of sputtering from either the metal or the stoichiometric compound phase. TRIDYN supports this option only for a substoichiometric compound of component no. 2 and component no. 3.

Experience indicates that the choice of the surface binding model influences the sputtering yields only to a minor extent, but may have a significant effect on the energy distributions of the sputtered particles.

In the following, recipes will be given for the choice of the surface binding energies and the matrix elements.

A2.3.1 Enthalpy of Sublimation

For the prediction of the sputtering yield of monoatomic substances, the choice of the sublimation enthalpies ΔH^s for the surface binding energies has proven to be successful:

$$sbe_i = \Delta H_i^s \qquad \text{(A3)}$$

This simple model is also a good approximation for multiatomic targets with low heats of fusion, such as metallic alloys, which is implemented by

$$sbv_{ij} = \Delta H_i^s \qquad \text{(A4)}$$

A2.3.2 Nonreactive Gaseous Components

It is often difficult to define the surface binding energy of a nonreactive gaseous component, due to the very low and often unknown enthalpy of physisorption. Ideally, one would tend to set

$$\Delta H_i^s \rightarrow 0 \qquad \text{(A5)}$$

However, this choice would require consistently low cutoff energies (see A3.1) and result in long computing times. A general recipe cannot be given. The stability of the results against the choice of the surface binding energy should be checked.

A2.3.3 Solid-Solid Compounds

For a diatomic solid-solid compound A_nB_m, conservation of energy requires

$$n \cdot sbe_A + m \cdot sbe_B = n \cdot \Delta H_A^s + m \cdot \Delta H_B^s + \Delta H^f \tag{A6}$$

with the enthalpy of fusion ΔH^f. Eq. (A2) reads

$$sbe_A = sbe_{AA}q_A + sbe_{AB}q_B$$
$$sbe_B = sbe_{BA}q_A + sbe_{BB}q_B \tag{A7}$$

As the matrix elements sbv_{ij} denote the interaction energies between atoms i and j, $sbv_{ij} = sbv_{ji}$ can be assumed. For $q_A = 1$ and $q_B = 0$ and vice versa, the pure components A or B are obtained, respectively, so that

$$sbv_{AA} = \Delta H_A^s$$
$$sbv_{BB} = \Delta H_B^s \tag{A8}$$

The combination of eqs. (A6,A7,A8) yields for the stoichiometric compound with $q_A = n/(n+m)$ and $q_B = m/(n+m)$

$$sbv_{AB} = sbv_{BA} = \frac{\Delta H_A^s + \Delta H_B^s}{2} + \frac{n+m}{2nm}\Delta H^f \tag{A9}$$

It should be noted that this linear formalism can only be a crude approximation of the real thermochemistry of the binary compound, which is best if the deviation from the stoichiometric compound is not too strong. Alternatively, by setting $q_A = 0$ and $q_B = 1$ in eq. (A7 top) or vice versa in eq. (A7 bottom) for the extremes far from stoichiometry, the non-diagonal matrix elements may be identified with the sorption energy of A on the elemental B surface, or vice versa, which are not symmetric in general. Then

$$sbv_{AB} = \Delta H_{AB}^{sorp}$$
$$sbv_{BA} = \Delta H_{BA}^{sorp} \tag{A10}$$

where $\Delta H^{sorp}{}_{ij}$ denotes the sorption enthalpy of atom i on the elemental surface j. Unfortunately, the sorption enthalpies are not readily available in literature, so one will generally prefer the approach of eqs. (A8,A10), except when treating specific problems of surface physics.

A2.3.4 Solid-Gas Compounds

If in a diatomic compound A_nB_m one of the components is from a diatomic gas, e.g., B, the energy conservation reads

$$n \cdot sbe_A + m \cdot sbe_B = n \cdot \Delta H_A^s + \Delta H^f + \frac{m}{2}\Delta H^{diss} \tag{A11}$$

where ΔH^{diss} denotes the dissociation enthalpy of the gas. One may neglect any interaction of B atoms with each other in the surface. (Otherwise, they would react and form a volatile molecule.) Therefore

$$sbv_{AA} = \Delta H_A^S$$

$$sbv_{BB} = 0 \tag{A12}$$

Then, the combination of eqs. (A6,A11,A12) yields for the stoichiometric compound

$$sbv_{AB} = sbv_{BA} = \frac{\Delta H_A^S}{2} + \frac{n+m}{2nm}\Delta H^f + \frac{n+m}{4n}\Delta H^{diss} \tag{A13}$$

Data of the matrix elements sbv_{ij} according to eqs. (A8,A9) and (A11,A12) are tabulated for standard binary compounds in an internal list of TRIDYN (see Appendix D for a list of available compounds).

A2.4 Relocation Threshold Energy, Subthreshold Recoils
The final relocation of a recoil atom, which is not sputtered, requires an initial energy transfer larger than the respective relocation threshold energies ed_i. The conventional model assumes that a interstitial-vacancy or Frenkel pair can only be formed if the interstitial atom is relocated far enough from its original lattice site, corresponding to the relocation threshold, which is in the order of several 10 eV. (In the simulation, all recoil atoms are followed down to their cutoff energy. "Subthreshold" recoils with a starting energy below the relocation threshold energy are restored at their original sites after cutoff. In this way, in the subthreshold regime only mass transport is suppressed, whereas cascade evolution and momentum transport are maintained. Thus, e.g., sputtering is not influenced by the choice of the relocation threshold.)
It should be noted that the above concept of a displacement threshold is strictly valid only for a perfect and non-damaged crystal. In an amorphous substance or in a solid being subjected to high-fluence ion bombardment, relocation thresholds might be significantly lower. Well-based data cannot be given. However, according to experience with ion mixing and preferential sputtering simulations and their comparison to experimental findings, a relocation threshold energy of 8 eV has turned out to be successful in a number of different systems, such as metallic compounds at low temperature and oxides, so that this value is recommended.

A3 Atomic Density

For monoatomic materials the atomic densities of the pure element can be used. In the case of compound materials, TRIDYN calculates the local total atomic density dns linearly from the atomic densities (or the inverse of the atomic volumes) of the individual components, $dns0_i$, according to

$$\frac{1}{dns} = \sum_{j=1}^{ncp} \frac{q_j}{dns0_j} \tag{A14}$$

Similar to the choice of surface binding energies (see sect. A2.2), in dependence on the actual problem it has to be decided which limiting cases shall be reproduced correctly. In a solid-solid compound with little chemical interaction, the choice of the pure element atomic densities for $dns0_i$ trivially reproduces the atomic densities of the pure elements and yields a good approximation for the whole range of concentrations.

In a highly covalent solid-solid compound or in a solid-gas compound, normally the density of the stoichiometric compound and that of one of the constituents should be reproduced correctly. (In a solid-gas compound, the atomic density of the pure gaseous component is ill-defined, anyway.) As above, the following recipe shall be restricted to a two-component compound A_nB_m. Starting from

the mass density ρ_A of the "principal" component A (the nongaseous component or the component for which the pure elemental density shall be reproduced correctly), and the mass density of the compound $\rho_{A_nB_m}$, the corresponding atomic densities are

$$dns0_A = \frac{\rho_A L}{M_A}$$

(A15)

$$dns_{A_nB_m} = \frac{\rho_{A_nB_m} L}{nM_A + mM_B}$$

with L denoting Avogadro's number and M the atomic masses. Then, the atomic density of the non-principal component is calculated from eq. (A14) according to

$$dns0_B = \left(\frac{n+m}{m}\frac{1}{dns_{A_nB_m}} - \frac{n}{m}\frac{1}{dns0_A}\right)^{-1}$$

(A16)

Note! For compounds with a very high atomic density, the atomic density of the non-principal component may become negative according to eq. (20). This represents no problem for the processing in the program.

Data of the inverse atomic volumes $dns0$ according to eqs. (A15,A16) and (A11,A12) are tabulated for standard binary compounds in an internal list of TRIDYN (see Appendix D for a list of available compounds).

A4. Energy of Incidence

Molecular Bombardment
In certain cases, the incident species are molecules, e.g., A_nB_m. For each of the constituents, the beam fractions and the incident energies have to be defined consistently. For incident energies being sufficiently large compared to the molecular binding energies, surface collisions will cause an immediate dissociation of the incident molecule. Then, the incident energy $e0_{A_nB_m}$ of the molecule is distributed according to the atomic masses M_A and M_B, resulting in the energies of A and B

$$e0_{A,B} = \frac{M_{A,B}}{nM_A + mM_B}e0_{A_nB_m}$$

(A17)

Correspondingly, the beam fractions *qubeam* of the components A and B are to be adjusted.

Appendix B

Beam angular distributions

The program supports two types of 2D axisymmetric beam angular distributions.

The actual direction of incidence is chosen randomly around the mean direction $\overrightarrow{d_{inc}}$ with an axisymmetric distribution $f(\Delta\alpha)$ over the polar angular variation $\Delta\alpha$ (see Fig. B1).
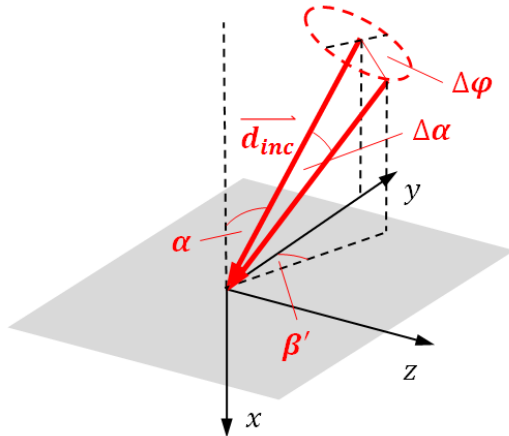

Figure B1: Irradiation geometry with a distributed angle of incidence. The actual direction of incidence is obtained from random choices of the polar angle $\Delta\alpha$ according to the predefined angular distribution, and the azimuthal angle $\Delta\varphi$. Depending on the random choices, the actual direction of incidence attains a component in z direction, represented by the angle β' in the $y - z$ plane.

B 1 Gaussian distribution

The Gaussian distribution (normalized to 1 at maximum) is given by

$$f(\Delta\alpha) = exp\left(-\frac{\Delta\alpha^2}{2\sigma^2}\right) \tag{B1}$$

with the standard deviation $\sigma = w_{HM}/2.355$ where w_{HM} is the full width at half maximum. As the Gaussian distribution extends to infinity, which would cause irradiation directions away from the surface, a cutoff angle α_0 (in multiples of σ) is entered as an additional parameter. Fig. B2 shows an example. Normally, the Gaussian distribution is employed to describe narrow angular beam profiles.
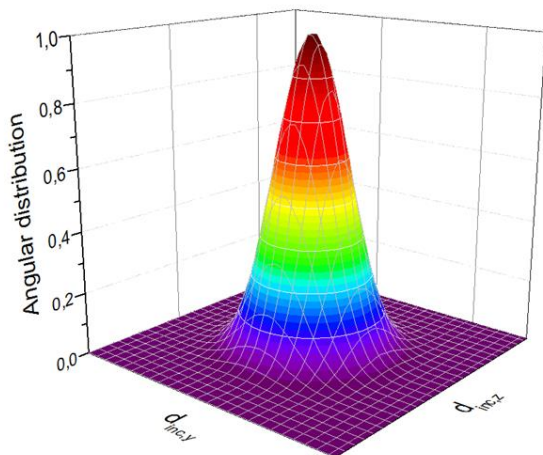

Figure B2: 2D Gaussian angular distributions with an FWHM of 30° and a cutoff angle of 4σ. (The latter is invisible in the plot.). For normal incidence, the distributions are plotted over the lateral components of the direction of incidence (or directional cosines) in y and z direction, both ranging from -1 to +1. The distribution has been generated from 10^7 random calls of the angular distribution routine.

B 2 Cosine^x distribution

The cosine^x distribution (normalized to 1 at maximum) is given by

$$f(\Delta\alpha) = cos^x\left(\frac{\pi}{2}\frac{\Delta\alpha}{\alpha_0}\right) \tag{B2}$$

with the exponent x. It vanishes at the maximum angle

$$\alpha_0 = \frac{\pi}{4}\frac{w_{HM}}{arccos\left(\left(\frac{1}{2}\right)^{\frac{1}{x}}\right)} \tag{B3}$$

with the full width at half maximum w_{HM}. Thus, it is defined by the two parameters x and w_{HM}. Examples are given in Fig. B3. With $x \rightarrow 0$, the profiles take a more box-like shape, with a cylindrical distribution at $x = 0$, whereas they flatten out for $x > 1$.

A special case is the "gas-kinetic" cosine distribution with $x = 1$ and $w_{HM} = 120°$, which describes the flow of a gas from a half-space, and can thus be applied to the simulation of neutral fluxes in, e.g., ion- or plasma-assisted deposition.
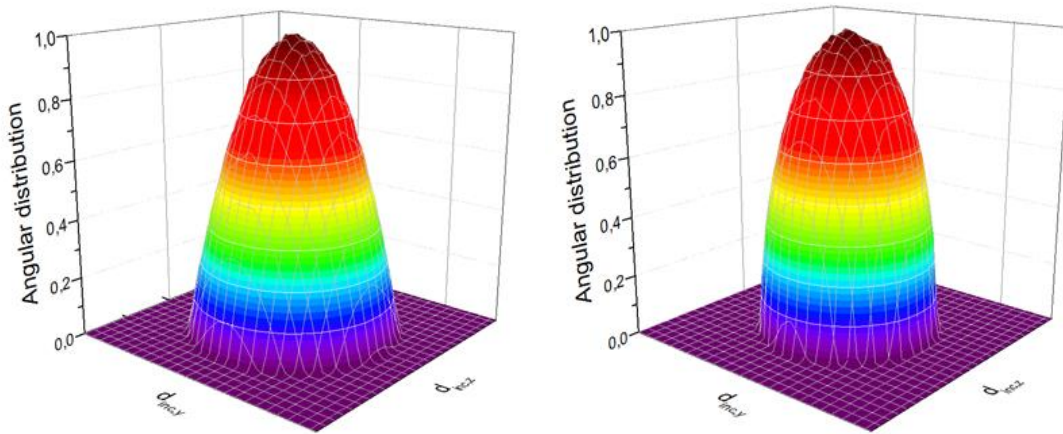

Figure B3: 2D cosine^x angular distributions at normal incidence, with a FWHM of 60° and exponents $x = 1$ (left) and $x = 1/2$ (right). See Fig. B2 for the lateral scales and the origin of the distributions.

Appendix C

List of available compounds

The internal compound list of TRIDYN covers the following binary compounds:

Hydrides, Polymers

CHps (= Polystyrene $(C_8H_8)_n$)

Borides

FeB, MgB_2, TiB_2

Carbides

Al_4C_3, TaC, SiC, TiC

Oxides

Al_2O_3, As_2O_3, B_2O_3, Cr_2O_3, Cs_2O, Fe_2O_3, Ga_2O_3, GeO_2, MgO, Mn_3O_4, P_2O_5, RuO_2, SeO_2, SiO_2, SnO_2, Ta_2O_5, TiO_2, UO_2, WO_3, ZnO, ZrO_2

Nitrides

AlN, cBN, hBN, CrN, HfN, Si_3N_4, TiN

Silicides

$CoSi_2$, $FeSi_2$, FeSi, $MgSi_2$, PtSi, $TiSi_2$, WSi_2

Arsenides

GaAs

Antimonides

GaSb